The Plant Cell, Vol. 27: 3294–3308, December 2015, www.plantcell.org

LARGE-SCALE BIOLOGY ARTICLE

Transcriptome-Wide Identification of RNA Targets of Arabidopsis SERINE/ARGININE-RICH45 Uncovers the Unexpected Roles of This RNA Binding Protein in RNA Processing[OPEN]

Denghui Xing,[a] Yajun Wang,[a] Michael Hamilton,[b] Asa Ben-Hur,[b] and Anireddy S.N. Reddy[a,1]

[a] Department of Biology and Program in Molecular Plant Biology, Colorado State University, Fort Collins, Colorado 80523
[b] Computer Science Department, Colorado State University, Fort Collins, Colorado 80523

ORCID ID: 0000-0003-0283-4247 (D.X.)

Plant SR45 and its metazoan ortholog RNPS1 are serine/arginine-rich (SR)-like RNA binding proteins that function in splicing/postsplicing events and regulate diverse processes in eukaryotes. Interactions of SR45 with both RNAs and proteins are crucial for regulating RNA processing. However, in vivo RNA targets of SR45 are currently unclear. Using RNA immunoprecipitation followed by high-throughput sequencing, we identified over 4000 *Arabidopsis thaliana* RNAs that directly or indirectly associate with SR45, designated as SR45-associated RNAs (SARs). Comprehensive analyses of these SARs revealed several roles for SR45. First, SR45 associates with and regulates the expression of 30% of abscisic acid (ABA) signaling genes at the postsplicing level. Second, although most SARs are derived from intron-containing genes, surprisingly, 340 SARs are derived from intronless genes. Expression analysis of the SARs suggests that SR45 differentially regulates intronless and intron-containing SARs. Finally, we identified four overrepresented RNA motifs in SARs that likely mediate SR45's recognition of its targets. Therefore, SR45 plays an unexpected role in mRNA processing of intronless genes, and numerous ABA signaling genes are targeted for regulation at the posttranscriptional level. The diverse molecular functions of SR45 uncovered in this study are likely applicable to other species in view of its conservation across eukaryotes.

INTRODUCTION

Most eukaryotic genes are interrupted by noncoding sequences (introns) that are excised with precision by the spliceosome, a large RNA-protein complex consisting of five small nuclear RNAs and over 300 proteins (Jurica and Moore, 2003; Hoskins and Moore, 2012). A large fraction of spliceosomal proteins assist the spliceosome in splice site recognition, regulate the number and types of mature mRNAs generated from a gene, and/or couple splicing with other aspects of RNA processing (Jurica and Moore, 2003; Kalsotra and Cooper, 2011; Hoskins and Moore, 2012). Serine/arginine-rich (SR) and SR-like RNA binding proteins function in both constitutive and alternative splicing (AS) of nuclear pre-mRNAs as well as other aspects of RNA metabolism in eukaryotes (Long and Caceres, 2009; Reddy and Shad Ali, 2011). *Arabidopsis thaliana* SR45 and its metazoan counterpart RNPS1 are SR-like proteins with two RS domains, flanking either side of the RNA recognition motif (RRM) (Badolato et al., 1995; Golovkin and Reddy, 1999; Ali et al., 2007; Singh et al., 2012). The domain organization and the RRM amino acid sequence of SR45 and RNPS1 are conserved across kingdoms (Califice et al., 2012). A phylogenetic analysis of RNA recognition domains from more than 100 species has shown that SR45/RNPS1 shares a single evolutionary origin with other SR proteins (Califice et al., 2012). The functions of RNPS1 are also largely conserved across species in spite of some diversification (Gatfield et al., 2003; Ashton-Beaucage et al., 2010; Roignant and Treisman, 2010). As in human RNPS1, both *Drosophila melanogaster* RNPS1 and Arabidopsis SR45 play a role in AS (Ali et al., 2007; Ashton-Beaucage et al., 2010; Roignant and Treisman, 2010) and both appear to be a component of the exon-exon junction complex (EJC) (Gatfield et al., 2003; Koroleva et al., 2009), a protein complex deposited at the exon-exon junctions as a result of splicing (Le Hir et al., 2001). RNPS1 is unique in that it participates in many aspects of splicing and postsplicing processes. In addition to regulating constitutive and alternative splicing (Mayeda et al., 1999; Sakashita et al., 2004; Michelle et al., 2012), RNPS1 plays a role in mRNA 3′-end formation (McCracken et al., 2003; Wiegand et al., 2003), subcellular localization and nuclear export of spliced mRNAs (Gatfield and Izaurralde, 2002; Li et al., 2003; Miyagawa et al., 2012), nonsense-mediated decay (NMD) (Lykke-Andersen et al., 2001), and enhancing translation (Wiegand et al., 2003; Nott et al., 2004). Recent studies have also revealed a role for SR45/RNPS1 in genome stability and RNA-directed DNA methylation (Li et al., 2007; Ausin et al., 2012).

The versatile functions of SR45/RNPS1 are due to its ability to interact with multiple proteins in distinct protein complexes, such

[1] Address correspondence to reddy@colostate.edu.
The author responsible for distribution of materials integral to the findings presented in this article in accordance with the policy described in the Instructions for Authors (www.plantcell.org) is: Anireddy S.N. Reddy (reddy@colostate.edu).
[OPEN]Articles can be viewed online without a subscription.
www.plantcell.org/cgi/doi/10.1105/tpc.15.00641

as the EJC and spliceosomal proteins that are not part of the EJC (Le Hir et al., 2000; Lykke-Andersen et al., 2001; Gatfield and Izaurralde, 2002; Li et al., 2003; Wiegand et al., 2003; Nott et al., 2004; Singh et al., 2012). SR45/RNPS1-interacting proteins such as Tra2β, SRSF6, and SART3 in humans (Harada et al., 2001; Sakashita et al., 2004) and U1 snRNP component U1-70K, SCL33, and SKIP in Arabidopsis (Golovkin and Reddy, 1999; Wang et al., 2012), likely mediate its function in splicing. Consistent with its role in splicing, SR45/RNPS1 associates physically with some pre-mRNAs (Mayeda et al., 1999; Lykke-Andersen et al., 2001; Day et al., 2012) and is found in early spliceosomes (Reichert et al., 2002; Kataoka and Dreyfuss, 2004; Trembley et al., 2005). A recent study has shown that both RNPS1 and EJC core proteins modulate AS of B-cell lymphoma-extra large (*Bcl-x*), which encodes a transmembrane molecule in the mitochondria (Michelle et al., 2012). However, different *cis*-elements mediate the action of RNPS1 and the EJC, further suggesting that the function of RNPS1 in splicing is likely through a protein complex that is distinct from the EJC (Michelle et al., 2012).

Previous studies of metazoan RNPS1 were largely based on in vitro splicing assays with a few model transcripts (e.g., β-globin pre-mRNA) or in vivo assays with reporter genes (Sakashita et al., 2004; Michelle et al., 2012). Some studies have shown clear substrate specificity for RNPS1 in modulating splicing. Overexpression of RNPS1 in HeLa cells promoted AS of β-*globin* and transformer 2 β-subunit (*Tra2β*) pre-mRNAs, but not mitochondrial ATP synthase γ-subunit ($F_1\gamma$) pre-mRNA (Sakashita et al., 2004). Human RNPS1 associates with a variety of apoptosis genes (Michelle et al., 2012) and, in particular, promotes the AS of the *Bcl-x* pre-mRNA. In Drosophila, RNPS1 regulates AS of a set of genes that contain long introns (Ashton-Beaucage et al., 2010; Roignant and Treisman, 2010). Similarly, the AS of some Arabidopsis SR genes is regulated by SR45/RNPS1 (Ali et al., 2007). In addition to splicing, RNPS1 might also exhibit targeting specificity for its EJC-mediated functions. For example, the nuclear export of poly (A) RNA was only partially affected by depletion of Dm-RNPS1 (Gatfield and Izaurralde, 2002); Hs-RNPS1 was preferentially associated with spliced integrin-linked kinase mRNA that was subjected to NMD and with unspliced pre-mRNA of *Bcl-x* that was subjected to AS (Michelle et al., 2012). A recent proteomic study revealed that Hs-RNPS1 is much less abundant than other proteins in the core EJC complex, suggesting that it selectively associates with some exon-exon junctions and, therefore, selectively directs the downstream processing of those mRNAs (Singh et al., 2012). The targeting specificity may be achieved through the presence of a combination of *cis*-elements within the transcripts and the RNA binding selectivity of SR45/RNPS1 and/or its interacting proteins. A few known SR45/RNPS1 interactors such as Tra2β, SRSF6, and SCL33 are RNA binding proteins with known or suggested binding selectivity (Nagel et al., 1998; Tacke et al., 1998; Golovkin and Reddy, 1999).

Despite strong evidence that SR45/RNPS1 has substrate specificity, few SR45/RNPS1-associated transcripts have been identified in vivo, with the exception of human *Bcl-x* and a reporter gene (Lykke-Andersen et al., 2001; Michelle et al., 2012). Identification of SR45-associated transcripts in vivo will facilitate our understanding of how it achieves its targeting specificity and, more importantly, will pave the way for the molecular understanding of its diverse functions. In this study, using RNA immunoprecipitation (RIP) followed by high-throughput sequencing (RIP-seq), we identified over 4000 Arabidopsis SR45-associated RNAs (SARs). Gene Ontology (GO) enrichment analysis of the SARs revealed SR45's function in regulating the expression of the genes in key nodes of the abscisic acid (ABA) signaling network at the postsplicing level. Sequence analysis of the SAR genes revealed four highly enriched RNA motifs that may mediate SR45's association with the SARs. The majority of SARs were derived, as expected, from intron-containing genes. To our surprise, 340 SARs were from intronless genes. Analysis of the SARs' expression suggests that SR45 employs different mechanisms in regulating intronless and intron-containing SARs. Our work reveals an unexpected role of SR45 in the processing of intronless mRNAs and indicates that the expression of many ABA signaling genes is regulated at the postsplicing level by SR45.

RESULTS

Arabidopsis SR45 Associates with Thousands of RNAs in Planta

Arabidopsis SR45 was first identified as an interactor of the U1 snRNP component U1-70K and was shown to function as a splicing factor using β-globin pre-mRNA in an in vitro splicing assay (Golovkin and Reddy, 1999; Ali et al., 2007). The loss-of-function mutation of *SR45* selectively altered the splicing of a set of genes and affected multiple aspects of plant development (Ali et al., 2007; Zhang and Mount, 2009). However, loss of *SR45* is not lethal under laboratory growth conditions (Ali et al., 2007; Zhang and Mount, 2009). Altered AS of some pre-mRNAs in the *sr45* mutant strongly suggests that SR45, as an RRM-containing protein, might associate selectively with some RNA transcripts in planta. Toward this end, we performed an RIP assay followed by high-throughput sequencing to identify genome-wide SARs.

SR45 is broadly expressed and alternatively spliced, producing two isoforms: *SR45.1* and *SR45.2* (Palusa et al., 2007). The two isoforms function differently, with *SR45.1-GFP* complementing the leaf and flower phenotypes in the mutant and *SR45.2-GFP* complementing the root phenotype (Ali et al., 2007; Zhang and Mount, 2009). Throughout this study, we used an *SR45.1-GFP* complemented line. The complementation was not attributed to the GFP tag since expression of GFP alone, which was expressed at an abundance similar to that of SR45.1-GFP (Figure 1A), did not cause any observable phenotypic effects on the transgenic plants. SR45.1-GFP thus mimicked the function of endogenous SR45. Consistent with previous studies showing that SR45, like Hs-RNPS1, is localized to nuclei (Mayeda et al., 1999; Ali et al., 2003, 2008), the SR45.1-GFP fusion protein was detectable in the nuclear extract from the complemented line (Figure 1A). The SR45.1-GFP fusion protein could be immunoprecipitated from the nuclear extract using anti-GFP antibody (Figure 1B). We therefore performed an RIP assay from the nuclear extract of *SR45.1-GFP* and wild-type Col (mock) plants using anti-GFP antibody. Figure 1C depicts the flow chart describing the steps followed to perform the RIP. Importantly, prior to RIP, we treated the Arabidopsis seedlings with formaldehyde to avoid adventitious

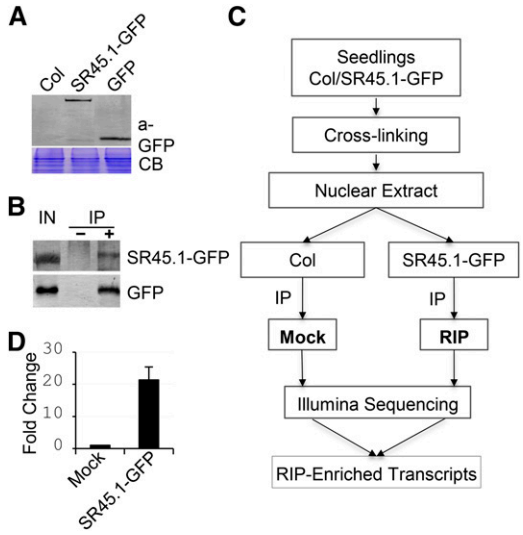

Figure 1. The RIP-Seq Procedure for Identification of SARs.

(A) Detection of SR45.1-GFP and GFP in nuclear extracts from transgenic plants using anti-GFP antibody (α-GFP). Col, wild-type Col-0; SR45.1-GFP, the mutant *sr45* complemented with 35S:SR45.1-GFP; GFP, transgenic line containing 35S:GFP. Coomassie blue (CB) staining shows similar amount of protein in all three samples.

(B) IP of SR45.1-GFP and GFP from nuclear extract with anti-GFP antibody (+) and a mock antibody (−). IN, input.

(C) Flowchart of the RIP-seq procedure and analysis. The immunoprecipitated RNA from Col (Mock) and SR45.1-GFP (RIP) was sequenced. Procedures used for mapping sequence reads and identification of a transcript as a SAR are described in Supplemental Figure 1.

(D) Enrichment of *SR34* transcripts measured by RT-qPCR. The data represent mean ± SD of three biological replicates.

RNA association with SR45.1-GFP after cell lysis (Figure 1C) (Mili and Steitz, 2004; Kaneko and Manley, 2005). The efficacy of RIP was monitored by the enrichment of the *SR34* transcript, an SAR candidate (Ali et al., 2007), relative to Mock treatment using an RT-qPCR assay (Figure 1D).

RNA that coprecipitated with SR45.1-GFP (RIP) and Col (mock) was sequenced using Illumina sequencing (Figure 1C). The sequence reads were of high quality, with 88 to 95% of the reads mapping to the TAIR10 genome (Supplemental Table 1). After removing duplicate reads and reads mapping to multiple genomic locations, an average of 6.8 million reads for RIP triplicates and 2.2 million for mock triplicates were further analyzed (Figure 2A; Supplemental Figure 1). The abundance of transcripts in each sample was measured by reads per kilobase per million (RPKM) (Supplemental Figure 1). The transcript abundance was more highly correlated between replicates of each sample than between RIP and mock (Figures 2B and 2C; Supplemental Figure 2). The enrichment of a given transcript in RIP was computed with Student's *t* test. The transcripts whose abundance showed significant difference between RIP and mock (adjusted $P < 0.05$) were further filtered based on their abundance level (RPKM > 20) and fold change (RIP/mock > 2) (Supplemental Figure 1). A total of 4361 transcripts derived from 4262 genes were identified and designated as SARs (Supplemental Figure 1 and Supplemental Data Set 1).

To verify the enrichment of the SARs with an independent method and to rule out the possibility that the enrichment was due to nonspecific binding of SARs to the GFP portion of SR45.1-GFP fusion, we performed RT-qPCR with RIP precipitated RNAs from SR45.1-GFP and GFP lines. The RIP enrichment of 16 out of 17 randomly selected SARs was further verified using RT-qPCR (Figure 2D). Strict filtering criteria and validation results suggest that the identified SARs are authentic targets of SR45.

A

Sample	Total reads	Multireads	Unique and non-duplicate reads
RIP1	39.5	22.8	7.78
RIP2	28.1	15.7	6.12
RIP3	41.0	27.0	6.59
Mock1	24.5	20.2	1.45
Mock2	44.8	37.2	2.42
Mock3	59.8	48.9	2.73

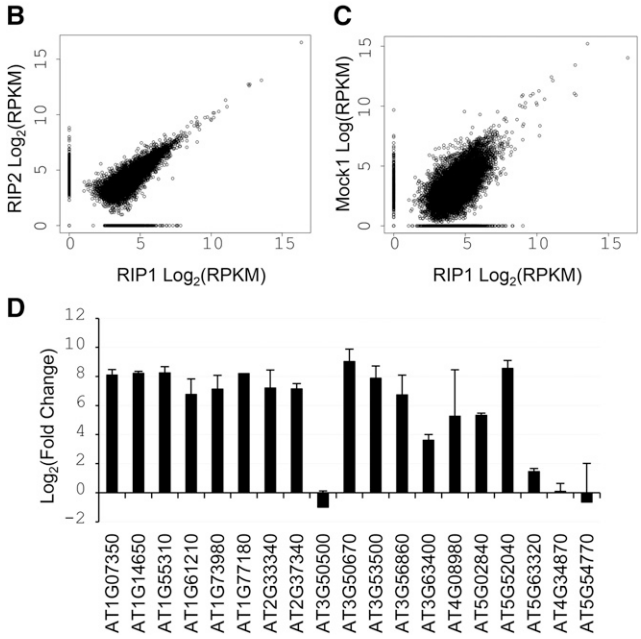

Figure 2. SR45 Associates with Thousands of RNAs (SARs) in Planta.

(A) Sequence statistics of immunoprecipitated RNA. The data represent millions of reads for three replicates each of SR45.1-GFP (RIP) and Col (Mock). Multireads, the number of reads mapped to multiple genomic regions; unique and nonduplicate reads, the number of reads after removing the multireads and duplicated reads due to PCR amplification.

(B) Dot plot of the $\log_2$ transformed RPKM (log(RPKM)) of all the detectable transcripts within RIP replicates (RIP1 versus RIP2).

(C) Dot plot of the $\log_2$ transformed RPKM (log(RPKM)) of all the detectable transcripts between RIP and mock (RIP1 versus Mock1).

(D) RT-qPCR verification of SAR enrichment. The enrichment was measured based on the fold change in immunoprecipitated RNA abundance in SR45.1-GFP compared with GFP line. The data represent mean ± SD of three biological replicates. The last two genes (AT4G34870 and AT5G54770) were not SR45 SARs and were used as negative controls.

GO Enrichment of SR45-Associated Transcripts Revealed SR45's Role in ABA Signaling Network

SR45 has been shown to play a role in plant development, possibly through regulating splicing, and to function in stress responses (Ali et al., 2003, 2007; Zhang and Mount, 2009; Carvalho et al., 2010). To see if SR45-associated transcripts mediate these functions, we performed a GO enrichment analysis with the SAR genes. Three methods, GeneCoDis, AgriGo, and DAVID, yielded similar results with a slight variation in the order of significance. Consistent with known functions of SR45, the SARs were indeed enriched in GO terms such as flowering, developmental growth, and RNA splicing (Supplemental Data Set 2). The most enriched terms are related to a variety of stress and hormonal responses (Figure 3; Supplemental Data Set 2). Of special interest was the GO term, response to ABA stimulus, for three reasons: (1) it was the most enriched GO term; (2) ABA has the most transcriptional targets in common with those of other hormones and plays a central role in stress responses (Nemhauser et al., 2006; Lee and Luan, 2012); and (3) SR45 was recently suggested to function in the ABA signaling pathway (Carvalho et al., 2010). Indeed, the *sr45* knockout mutant was hypersensitive to ABA treatment and showed a significant reduction in root growth, which was partially restored by the transgene *SR45.1-GFP* (Figures 4A and 4B). Since the ABA signaling pathway is involved in multiple biological processes, including seed germination, cotyledon greening, and drought tolerance, we further characterized the response of the *sr45-1* mutant in these aspects. The cotyledon greening of the *sr45-1* mutant was delayed about 2 d compared with both Col and *SR45.1-GFP*, even without ABA treatment (Supplemental Figure 3A). In the presence of 1 μM ABA, the delay was ~4 d, suggesting that ABA enhanced the delay in the *SR45* mutant (Figure 4C; Supplemental Figure 3A). The germination of the *sr45-1* mutant was not affected under normal growth conditions (Supplemental Figure 3B). The mutant, Col, and *SR45.1-GFP* lines all reached 100% germination in 3 d without ABA present in the medium. However, with increased ABA concentration in the medium, the germination rate of the *sr45-1* mutant was significantly higher than that of Col and *SR45.1-GFP*, suggesting that the mutant was less sensitive to ABA (Supplemental Figure 3B). To investigate if SR45 plays a role in drought tolerance, we tested the water loss in wild-type, *sr45-1* mutant, and complemented line using detached leaves (Hua et al., 2012). The mutant lost water much faster than wild-type and *SR45.1-GFP* lines (Figure 4D), suggesting that SR45 likely plays a positive role in Arabidopsis drought tolerance. Together, the results indicate that SR45 indeed plays a role in the ABA signaling pathway.

SR45 Regulates the Expression of Key ABA Signaling Genes at the Postsplicing Level

With the identification of the ABA receptors in the past few years, each node of the ABA signaling network has largely been defined (Hauser et al., 2011). Of the 147 genes identified in this network (Hauser et al., 2011), 43 of them were found among SARs (Supplemental Data Set 3). The SARs were particularly enriched in genes encoding phosphatase and kinase and transcription factors, two major hubs within the network (Figure 5A; Supplemental

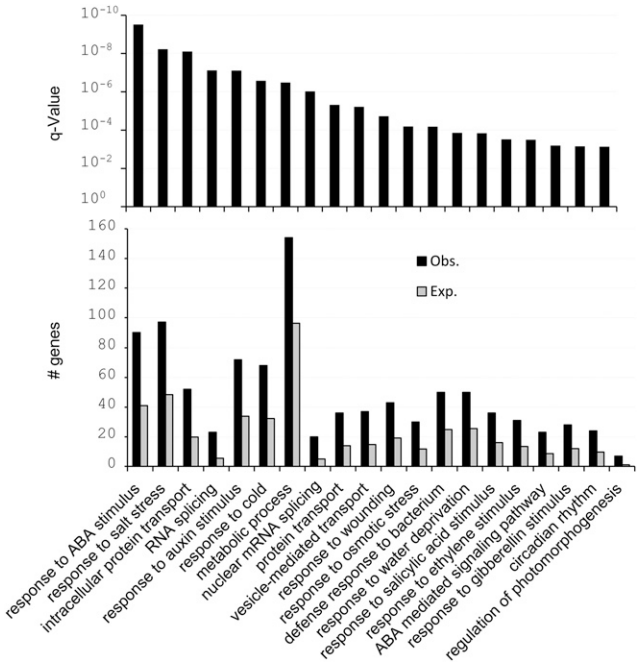

Figure 3. SAR-Encoding Genes Enriched in Hormonal and Stress Response Pathways Based on GO Analysis.

The statistical significance for the enrichment is presented in the upper panel (q-value, false discovery rate), and the expected (Exp.) and observed (Obs.) gene numbers for each GO term are presented in the lower panel.

Table 2) (Hauser et al., 2011), suggesting that the key ABA signaling genes are targeted for regulation by SR45. This regulation is likely at the posttranscriptional level since (1) RNPS1 is known for its role in splicing and postsplicing events; (2) most of the SAR genes have more than one isoform, evidenced by gene models, cDNAs, and ESTs from the TAIR10 database (Supplemental Table 3); and (3) the nuclear RNA sequence profiles for several of the SAR genes were altered in the *sr45-1* mutant (Supplemental Figure 4 and Supplemental Table 3).

The molecular phenotypes of the SARs in the *sr45* mutant may differ depending on which mRNA processing step (e.g., AS, nuclear export, NMD, or 3′end formation) of these SARs is affected by SR45. Therefore, the quantification of the total and individual isoforms of a given SAR may provide mechanistic insights into the affected processing step(s). Toward this end, we chose *HAB1* (encoding a PP2C phosphatase) as an example and quantified the abundance of its total transcripts and the abundance of its alternatively spliced isoform in the total cellular RNA fraction using RT-qPCR (Figure 5B). The tested AS isoforms were chosen based on two factors: (1) whether the isoform was the one affected the most by SR45 mutation based on our nuclear RNA-seq data (Supplemental Figure 4) and (2) whether the isoform was amenable to RT-qPCR measurement (i.e., a pair of primers could be designed to uniquely target the isoforms). As shown in Figure 5C, the total amount of the *HAB1* transcript was significantly reduced in the *sr45* loss-of-function mutant. This reduction was restored to the wild-type level in the *SR45.1-GFP* complementation line, indicating that the reduction was caused by the absence of SR45.

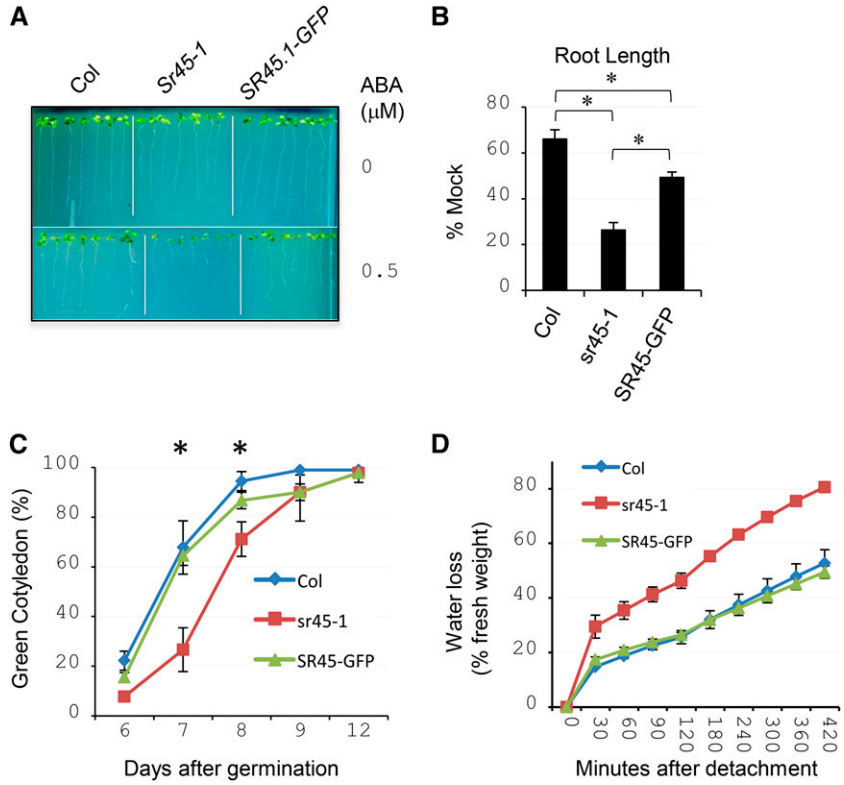

Figure 4. The SR45-Associated RNAs Reveal SR45's Function in the ABA Response.

(A) ABA treatment. Col, wild-type plants; SR45.1-GFP, the *sr45-1* mutant complemented with SR45.1-GFP. Pictures were taken 11 d after germination.
(B) The quantification of root growth of *sr45* under ABA treatment. The root length with ABA treatment was normalized to root growth without ABA treatment (Mock). The data represent mean ± SD of three biological replicates (n = 30). Asterisks denote significant difference ($P < 0.01$).
(C) The cotyledon greening of *sr45* with 1 μM ABA treatment. The data represent the mean ± SD of three biological replicates (n = 30 for each replicate). Asterisks denote significant difference ($P < 0.01$) between *sr45* mutant and Col or SR45.1-GFP.
(D) Water loss in the *sr45* mutant. The data represent the mean ± SD of three biological replicates (n = 12 for each replicate).

By contrast, the loss of SR45 increased the abundance of a splice variant of *HAB1* exhibiting intron retention, having the opposite effect on the total transcript level (Figure 5C). This effect was observed regardless of treatment with or without ABA (Figure 5C).

To see if this effect occurred with other ABA pathway genes, we analyzed an additional seven SAR genes in the ABA signaling network (Supplemental Figures 4 and 5). Although not every gene followed the exact pattern of the *HAB1* transcripts (e.g., ABA receptor gene *PYR1* and protein kinase gene *SnRK2.2*), the effect of SR45 mutation on the abundance of total transcripts was indeed negatively correlated with its effects on the AS isoform (Figure 5D, left panel; Supplemental Figure 5). The negative correlation might reflect an SR45-mediated coupling between transcription and splicing since it is known that RNA polymerase (Pol) II processivity is negatively correlated with AS (Nogués et al., 2003). Under this consideration, decreased Pol II processivity, which would lead to a reduced level of total transcripts, favors the use of alternative splice sites, resulting in increased levels of AS isoforms. Conversely, increased Pol II processivity would favor the skipping of the AS site, leading to increased levels of total transcripts and decreased levels of AS isoforms. Since the coupling was a nuclear event, the negative correlation between total transcript levels and AS should be more obvious in the nuclear RNA fraction. Alternatively, the negative correlation could be a result of altered stability (e.g., due to NMD) of a particular splicing isoform, which predominantly occurs in the cytosol (Popp and Maquat, 2013). In this case, the negative correlation could be better reflected in the cytosolic fraction. To distinguish between these two possibilities, the same experiments were performed using nuclear and cytosolic RNAs for those SAR genes. To ensure that the nuclear and cytosolic fractions were free or nearly free of cross-contamination from each other, we gauged the purity of each fraction with RT-qPCR and immunoblotting. To check the purity of the cytosolic fraction, the relative abundance of small nucleolar RNA U3 was measured (Kim et al., 2009), while the abundance of the cytosolic protein plastocyanin was probed to test the purity of the nuclear fraction (Abdel-Ghany et al., 2005). The level of U3 in the cytosolic fraction was one-fifteenth that in the nuclear fraction (Supplemental Figure 6A). Similarly, no plastocyanin was detectable in the nuclear fraction (Supplemental Figure 6B). Together, these results indicate that both fractions were sufficiently pure for testing the hypothesis. As shown in Figure 5D (middle panel) and Supplemental Figure 7, the negative correlation disappeared in the nuclear RNA and was strongly

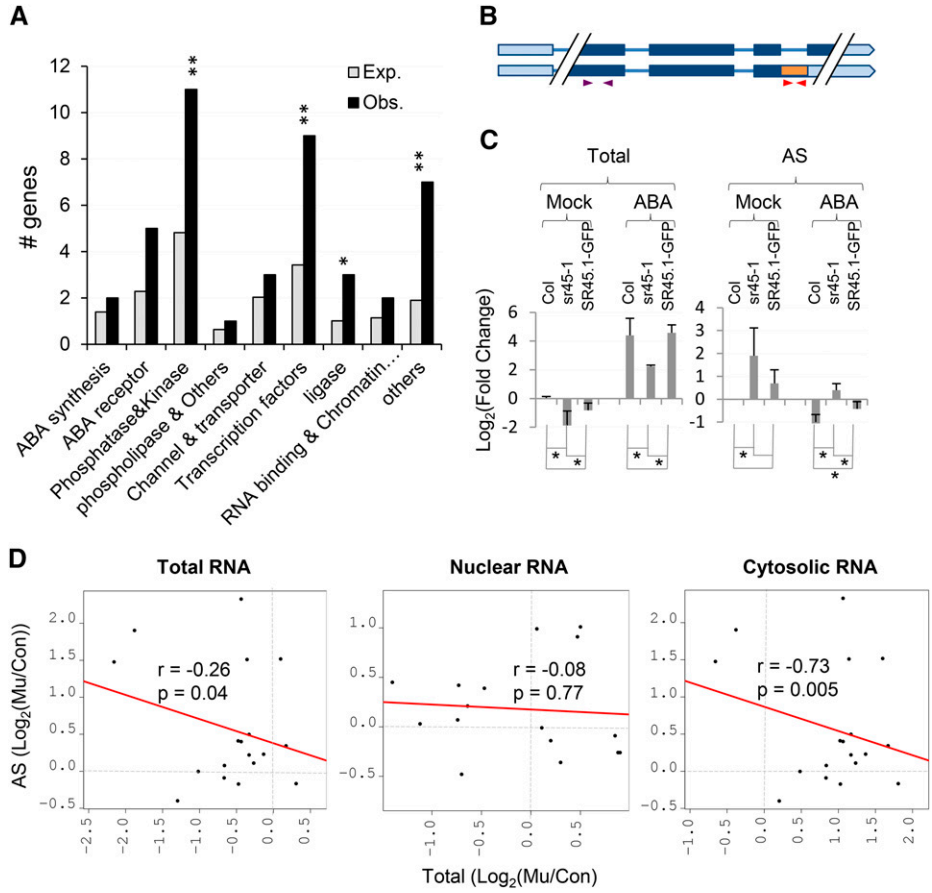

Figure 5. SR45 Regulates the Expression of Key Components of the ABA Signaling Network at the Postsplicing Level.

(A) SARs involved in response to ABA stimulus are enriched in particular nodes of the ABA signaling network. Obs., number of genes observed; Exp., number of genes expected; single and double asterisks denote significance levels at $P < 0.001$ and $P < 0.01$, respectively.

(B) The two splice variants of *HAB1*. The light-blue bars represent 5′ and 3′ untranslated regions, the dark-blue bars indicate the coding sequence, the lines represent introns, and the orange bar shows the retained intron. The arrows represent the primer pairs for quantification of total transcripts (purple, left) and the isoform with the retained intron (red, right) in **(C)**.

(C) RT-qPCR quantification of the total transcripts (Total) and the intron-containing isoform (AS) of *HAB1* under ABA and mock treatment. The data were relative to that of wild-type Col under mock treatment. The data represent mean ± SD of three biological replicates. Asterisks denote the significant difference ($P < 0.05$) based on *t* statistics.

(D) The effect of SR45 mutation on the isoforms in the total, nuclear, and cytosolic RNA. The effect was measured by the abundance change of the transcripts in *sr45* (Mu) relative to wild-type Col (Con): $\log_2$(Mu/Con)). The data points represent the average change of three biological replicates for total or isoform of each gene. A total of 18 data points from nine genes were used for each correlation assay.

enhanced in the cytosolic RNA fraction (Figure 5D, right panel; Supplemental Figure 8). These results support the latter mechanism that the major effect of SR45 on these SARs was on the selective stability of particular isoforms in the cytosol. The fact that the total expression of only 6 of the 147 ABA responsive genes showed differences in nuclear RNA levels between SR45.1-GFP and the *sr45-1* mutant further supports this conclusion (Supplemental Data Sets 3 and 4).

The Selective Association of SR45 with SARs Is Likely Defined by *cis*-Elements within the SAR Sequences

Of the 16,169 genes with detectable expression (defined as genes with RPKM > 5 in the nuclear RNA sequence data of SR45.1-GFP), only 4361 RNAs were associated with SR45, suggesting that the SARs may share unique sequence feature(s) that mediate the specific association with SR45. To identify such *cis*-elements, we performed a MEME analysis (Bailey et al., 2009) using the SAR gene sequences as input and the sequences of highly expressed, non-SAR genes as a background. We used sequences of SAR genes instead of SAR transcripts for the analysis since the association of SR45 and other EJC components with certain transcripts is attributed to the early splicing events where sequence features within introns are critical (Michelle et al., 2012). This analysis revealed four significantly overrepresented RNA motifs within SAR gene sequences (Figure 6A; Supplemental Table 4). The motifs M1 and M4 are similar to the binding motifs of two metazoan splicing regulators, Tra2 and SRSF10, respectively

(Figure 6A; Supplemental Table 4) (Tacke et al., 1998; Feng et al., 2009; Cléry et al., 2011). M1 and M4 are also G/A rich and largely positioned within exons (Supplemental Figure 9A), which are the typical features of exonic splicing regulators that often mediate regulated splicing by SR proteins (Fairbrother et al., 2002). In contrast, M2 and M3 are T/C rich motifs and exhibit peaks in the intronic region of 5′ and 3′ splice sites (Figures 6A and 6B). A broader peak of M2 and M3 ~50 to 80 bases upstream of 3′ splice sites was also observed (Figure 6B). In addition, M2 and M3 also exhibited a biased distribution toward the 5′ transcription start site, while M1 and M4 were biased away from transcription termination sites (Supplemental Figure 9B). It will be interesting to see if these motifs indeed play a role in recruiting SR45 to the SARs.

To examine if a unique set of *cis*-elements might mediate association of SR45 with the intronless SARs, we performed the MEME analysis with the sequences of intronless SAR genes as input and the sequences of all expressed non-SAR intronless genes as a background. We found one enriched *cis*-element, highly similar to M1 discovered in all SAR gene sequences, suggesting that the same *cis*-element mediates SR45 association with intronless SARs as with a potential subset of SARs derived from intron-containing genes (Supplemental Figure 9C).

SR45 Associates with Transcripts Derived from Both Intron-Containing and Intronless Genes

SR45/RNPS1 is known to function in splicing and postsplicing processes (Golovkin and Reddy, 1999; Mayeda et al., 1999; Tange et al., 2004; Ali et al., 2007; Michelle et al., 2012). It is therefore expected that SR45 would be associated with transcripts from intron-containing genes. While the majority of SARs were indeed from intron-containing genes, surprisingly, 340 of the SARs were found to be from intronless genes (Figure 7A; Supplemental Data Set 5). The intronless genes are indeed "intronless," not merely based on annotation, but also because no spliced reads were aligned to them. These results clearly indicate that SR45 plays a role in the mRNA metabolism of intronless genes. Nevertheless, SR45's major function is likely in splicing or splicing-coupled events in intron-containing genes, since the intronless SARs were significantly underrepresented, while those of intron-containing genes were overrepresented in the SARs (Figure 7B).

SR45 Differentially Regulates the Expression of Intron-Containing and Intronless SAR Genes

To investigate the effect of SR45 on its SARs, the nuclear RNA from SR45.1-GFP and the *SR45* knockout mutant, *sr45-1*, was also sequenced (Supplemental Table 1). A genome-wide comparison between the nuclear transcriptomes of *SR45.1-GFP* and *sr45-1* was performed for each TAIR10 gene. The expression of 1223 genes was altered in the mutant, with 918 being differentially expressed (DE) and 331 being differentially processed (DP) (Supplemental Data Sets 4 and 6). Of the 1223 affected genes in the mutant, 116 are SAR genes, accounting for only a fraction of the total SAR genes (Figure 7D), indicating that the SR45 association per se is not sufficient to change steady state levels of the majority of its SARs under the current experimental condition. SR45 is known to function in a variety of stress responses and in

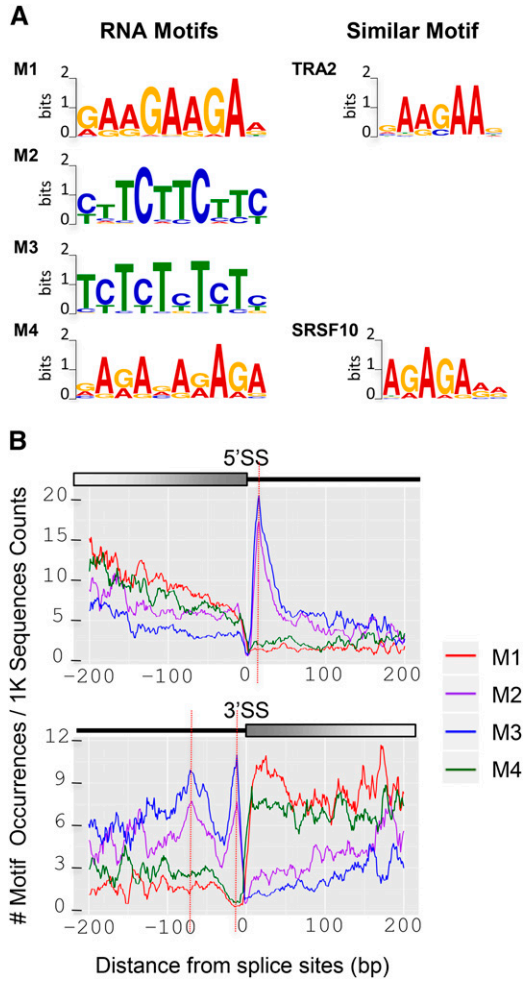

Figure 6. Overrepresented *cis*-Elements in SAR Genes.

The SAR gene sequences were analyzed using MEME with non-SAR gene sequences as background.

(A) Four *cis*-elements (RNA motifs), M1 to M4, are highly overrepresented in SAR sequences and showed similarity to known RNA binding motifs (Similar Motifs). The information content (bits) of each position is shown on the *y* axis. Tra2, Tra2 binding motif; SRSF10, SRSF10 binding motif.

(B) The distribution of each *cis*-element relative to 5′ (5′SS) and 3′ (3′SS) splice sites is mapped. M1 and M4 are more enriched in the exons than introns, whereas M2 and M3 exhibited peaks (red vertical lines) in the vicinity of splicing sites within the intron. The open bar on the top of each panel represents exon; the solid black line represents intron.

the circadian clock (Reddy and Shad Ali, 2011; Wang et al., 2012; Filichkin et al., 2015). Thus, it is possible that the effects of SR45 association with some of the SARs will be manifested only under those conditions. Although the transcript abundance of only a fraction of the SAR genes (116 out of 4262) was affected by *SR45* mutation, the DP genes remained significantly overrepresented among SARs (Figure 7C), suggesting that the effects of SR45 on those genes are likely more direct than indirect.

To investigate if SR45 might have a differential effect on its intronless and intron-containing SARs, the overlap of SR45 associated DE genes in these two categories was examined

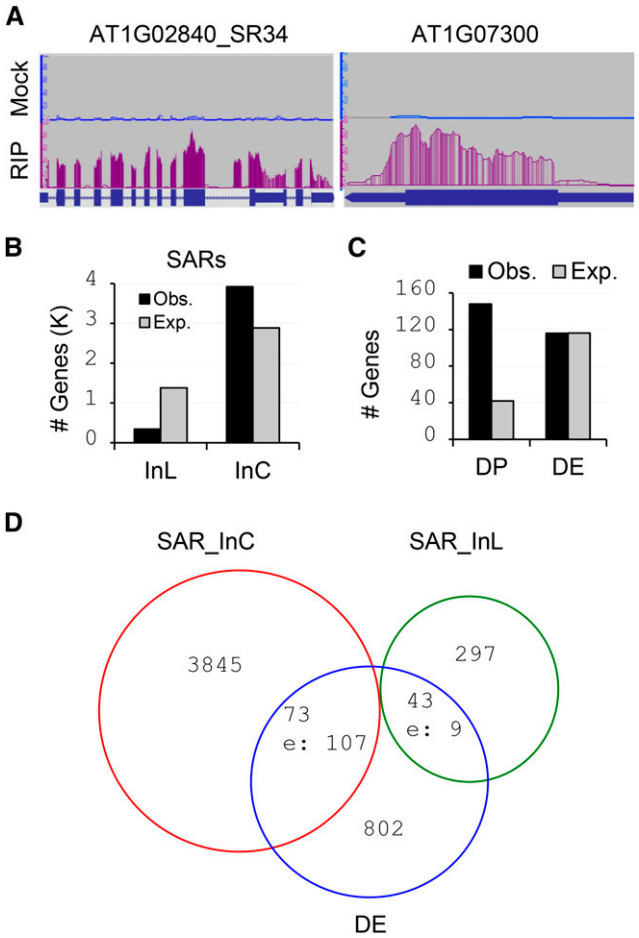

Figure 7. SR45 Associates with and Affects SARs from Both Intronless and Intron-Containing Genes.

(A) Integrated Genome Browser visualization of the sequence profiles of two representative SARs for one intron-containing gene (AT1G02840) and one intronless gene (AT1G07300). The relative sequence read abundance for each part of the gene is shown as histograms (purple for RIP; blue for mock). The *y* axis indicates the read depth with the same scale for both RIP and mock. The gene structures are illustrated under the sequence profile. The lines represent introns and the boxes represent exons. The thinner boxes represent 5′ and 3′ untranslated regions and AS regions.

(B) The intronless (InL) and intron-containing (InC) genes are not equally represented among the SAR genes. InL genes are underrepresented while intron-containing genes (InC) are overrepresented among SARs. Exp, expected number of genes; Obs, observed number of genes. The bias was significant based on χ^2 statistics (P = 1.45E-156).

(C) The effects of SR45 association with its SARs are greater on their processing than their total abundance. The DP, but not DE, genes in *sr45* are overrepresented among SARs based on χ^2 statistics (P = 9.6E-69 for DP genes; P = 0.97 for DE genes). Exp, expected number of genes as SARs; Obs, observed number of genes as SARs.

(D) The DE SAR genes are significantly biased to intronless SARs (SARs-InL) and biased away from intron-containing SARs (SAR-InC) based on χ^2 statistics (P = 6.9E-31). e:, expected number.

(Figure 7D). The DE genes were significantly biased toward the intronless SARs and biased away from intron-containing SARs (Figure 7D), suggesting that SR45 indeed affects its intronless and intron-containing SAR genes differentially. For the former, their transcript levels were affected, while for the latter, presumably, their processing was largely affected.

SR45 Affects the Expression of Intronless SAR Genes through Multiple Mechanisms

Of the 43 intronless DE genes associated with SR45, 27 of them showed a reduced abundance while 16 increased in abundance in the *sr45-1* mutant (Supplemental Data Set 7). Since the comparison was performed using nuclear RNA, the altered abundance level may reflect altered total abundance, altered nuclear export, or both. To discern between these possibilities, the transcript levels of a subset of nine genes, with seven showing decreased and two showing increased abundance in the mutant, were further examined in both nuclear and cytosolic RNA fractions. The RT-qPCR results verified their altered abundance in the nuclear RNA fraction of *sr45-1* compared with those of the SR45.1-GFP line and Col (with the exception of AT3G50060 in which the mutant was not significantly different from Col) (Figure 8). However, the change of their transcript abundance in the cytosol varied. For the two genes (AT5G18030 and AT5G18020) whose abundance increased in the nuclear fraction of the mutant, the increase was also observed in the cytosol fraction (Figure 8). On the other hand, the difference in transcript levels for the genes that showed significant reduction in the nuclear fraction of the mutant was largely diminished in the cytosol fraction (Figure 8). Together, the results indicate that the mechanisms with which SR45 affects its intronless SAR targets might be gene-specific.

DISCUSSION

SR45/RNPS1, an SR-like RRM-containing protein and an auxiliary component of the spliceosome, plays multiple roles in pre-mRNA splicing and postsplicing processes (Golovkin and Reddy, 1999; Mayeda et al., 1999; Sakashita et al., 2004; Tange et al., 2004; Ali et al., 2007; Zhang and Mount, 2009; Day et al., 2012; Michelle et al., 2012). Its functional versatility is likely manifested by its ability to interact with other proteins through its RS domains and RNAs through its RRM domain (Golovkin and Reddy, 1999; Le Hir et al., 2001; Lykke-Andersen et al., 2001; Sakashita et al., 2004; Day et al., 2012; Michelle et al., 2012; Thomas et al., 2012; Wang et al., 2012). While an array of proteins have been shown to possibly form distinct complexes with SR45/RNPS1, only a few RNAs are known to be associated with RNPS1 in vivo (Lykke-Andersen et al., 2001; Wiegand et al., 2003; Michelle et al., 2012). Here, we provide a comprehensive inventory of RNA targets associated with Arabidopsis SR45 in planta (Supplemental Data Set 1). Further examination of the SR45 targets revealed their diversity in processing status (spliced versus unspliced), in the structure of their coding genes (intron-containing versus intronless), and in their functions (significantly enriched in 111 GO terms) (Figures 3 and 7; Supplemental Data Set 2). While the majority of the SARs are from intron-containing genes, surprisingly, a significant portion of SARs corresponds to intronless genes. The

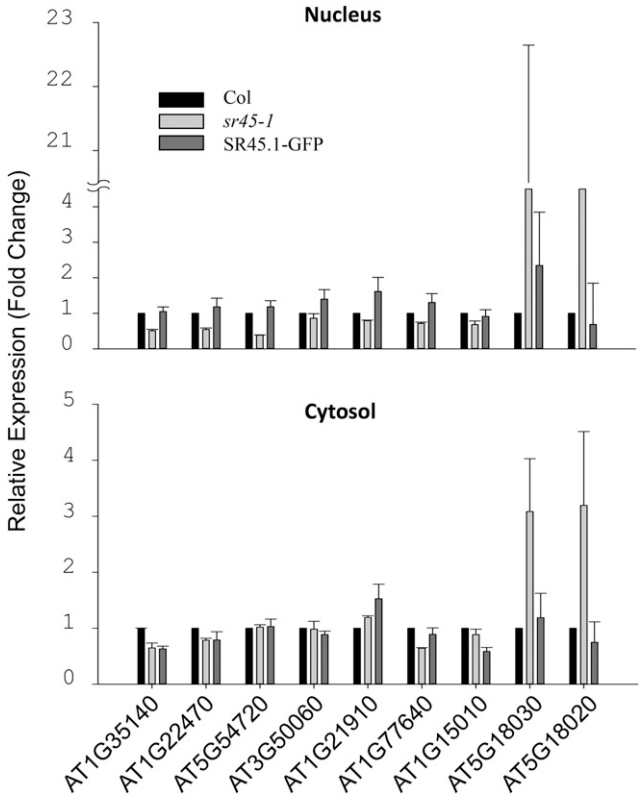

Figure 8. Verification of SR45-Associated Intronless DE Genes.

The down- and upregulated SR45-associated intronless DE genes were quantified using RT-qPCR from nuclear (Nucleus) and cytosolic (Cytosol) RNA fractions. The data represent mean ± SD of three biological replicates.

majority of SARs from intron-containing genes are spliced mRNAs (Figure 7A), likely reflecting the roles of SR45 in postsplicing processes as a component of the Arabidopsis EJC and/or other complexes (Tange et al., 2004; Brogna and Wen, 2009). On the other hand, the association of SR45 with unspliced pre-mRNAs or partially spliced mRNAs may indicate a role of SR45 in splicing (Ali et al., 2007; Ashton-Beaucage et al., 2010; Roignant and Treisman, 2010; Day et al., 2012; Michelle et al., 2012).

The association of SR45 with a significant portion of SARs from intronless genes was unexpected. However, the potential of RNPS1 forming an RNP complex with intronless mRNAs had been suggested previously. In a study of the effects of RNPS1 on the expression of the β-globin gene, the authors tethered RNPS1 to an intronless β-globin reporter through the B box and used the same β-globin gene lacking the B box as a control (Wiegand et al., 2003). Surprisingly, the expression of the control β-globin gene was also promoted by overexpression of RNPS1 (Wiegand et al., 2003). The stimulation was substrate-specific since no stimulation was observed with another intronless reporter, CAT mRNA (Wiegand et al., 2003). The authors hypothesized that there could be an RNPS1 binding site within the intronless β-globin mRNA that specifically mediates the RNPS1 stimulation effect (Wiegand et al., 2003). In support of this speculation, an earlier study also suggested that a *cis*-element within the β-globin mRNA mediates NMD independent of splicing (Zhang et al., 1998). Indeed, RNPS1 physically associates with intronless β-globin mRNA in vivo based on an RNase protection assay (Lykke-Andersen et al., 2001). Together, these studies suggest that Hs-RNPS1 binds to the intronless reporter β-globin mRNA in vivo and that the binding is independent of splicing. In addition to the intronless β-globin reporter, a recent study suggested that RNPS1 also forms an RNP complex with an endogenous interferon alpha1 (*IFN-a1*) mRNA, encoded by an intronless gene, based on yeast-three hybrid and subcellular colocalization assays (Kimura et al., 2010). In light of these reports and based on our global analysis results with Arabidopsis SR45, which show that this protein associates in planta with hundreds of mRNA from intronless genes, we propose that human RNPS1 may associate with more intronless mRNAs in vivo.

In an attempt to understand how SR45 might affect its intronless targets, we examined the molecular phenotypes of the SARs in both nuclear and cytosolic fractions using RT-qPCR. Loss of *SR45* caused altered abundance either in the nuclear fraction alone or in both fractions (Figure 8), suggesting that SR45 affects its intronless SARs differentially. Metazoan RNPS1 is known to affect the 3′ end cleavage of intronless β-globin reporter (Wiegand et al., 2003), and it also plays a role in the nuclear export of intronless *IFN-a1* mRNA (Kimura et al., 2010). It will be interesting to see if any of these mechanisms might operate in the case of SR45-associated intronless SARs, which would lead to the observed molecular phenotype. An RNA tethering assay might help resolve these potential mechanism(s).

The four highly enriched *cis*-elements in SARs likely define the target specificity of SR45. All four motifs are present in the majority of SAR genes (Supplemental Table 4). It is therefore possible that either one or more than one motif together define the association of SR45 with each SAR transcript. It is possible that additional motifs might exist within the subsets of SAR gene sequences that could not be discerned by the current analysis methods. Three recent studies in plants have revealed that the GAAG motif, which is similar to M1 in both exons and introns, is an important *cis*-element in regulating alternative splicing (Pertea et al., 2007; Thomas et al., 2012; Wu et al., 2014). Enrichment of this motif in SARs and SR45's interaction with key proteins involved in 5′ and 3′ site selection (Golovkin and Reddy, 1999; Day et al., 2012) suggest that SR45 is an important regulator of splicing. Analysis of intronless SAR genes with MEME revealed G/A-rich motifs similar to those in M1 and M4, suggesting that the discrimination of intronless and intron-containing SARs for the SR45 association is not likely defined by these two motifs. The predominant localization of M2 and M3 within introns supported our hypothesis that *cis*-elements within introns might be critical for the SR45 association with spliced mRNAs. An in vitro study has shown that SR45 can bind directly to a specific region of an intron in a pre-mRNA of an SR protein, whose splicing pattern is altered in the *sr45* mutant (Day et al., 2012). Another recent study has also shown that SR45 binds to an alternatively spliced intron of pre-mRNA, which encodes a key regulator of the circadian clock (Filichkin et al., 2015).

The list of SARs represents both direct and indirect targets of SR45. It is likely that some of the identified SARs are indirect targets, as SR45 has been shown to interact with other

spliceosomal proteins with RNA binding domains (e.g., SCL33, U2AF35, and U1-70K) or without RNA binding domains (e.g., AFC2 protein kinase and SKIP) (Golovkin and Reddy, 1999; Day et al., 2012; Wang et al., 2012; Zhang et al., 2014). Interestingly, one of the enriched *cis*-elements in SARs (GAAG element in M1) is the element through which SCL33 binds the pre-mRNA of Arabidopsis SCL33 in in vitro studies (Thomas et al., 2012). U2AF35, the small subunit of the U2AF complex involved in the recognition of 3′ splice sites (Wu et al., 1999; Zorio and Blumenthal, 1999; Day et al., 2012), which are rich in pyrimidines, also interact with SR45. In fact, two of the four enriched motifs (M3 and M4) are rich in pyrimidines. These studies support the assumption that some of the SARs are likely indirect targets of SR45. Analysis of RNA targets using tools such as photoactivatable-ribonucleoside-enhanced cross-linking and immunoprecipitation in the future should allow us to distinguish between direct and indirect targets of SR45. A recent study in humans revealed a complicated interaction between splicing regulators and the RNA binding motifs within introns (Wang et al., 2013). The study showed that a single RNA binding motif could be recognized by multiple splicing regulators and vice versa, forming a complicated regulatory network. SR45 may bind the enriched motifs directly or, alternatively, its association with these motifs might be mediated by other proteins known to interact with SR45 (Golovkin and Reddy, 1999; Day et al., 2012; Wang et al., 2012; Zhang et al., 2014). Together, the multiple interacting proteins of SR45, the number of motifs, and the varied positions of these motifs within the SARs might explain the diverse effects of SR45 on its SARs described above.

In spite of its role in Arabidopsis development, SR45 is dispensable for the completion of the life cycle under laboratory growth conditions (Ali et al., 2007; Zhang and Mount, 2009), suggesting that it may also be involved in other functions. Consistently, the GO terms related to development are, while enriched, not the most enriched of the SARs (Supplemental Data Set 2). On the other hand, the most enriched GO terms are largely related to stress and hormonal responses (Figure 3; Supplemental Data Set 2), indicating other major functions of SR45 in plant adaptation to its environments. Indeed, SR45 is suggested to function in multiple abiotic stress responses, such as hypoxia and ABA responses (Ali et al., 2003; Koroleva et al., 2009; Carvalho et al., 2010).

The ABA signaling network is regulated at multiple levels, such as transcription and protein phosphorylation/dephosphorylation (reviewed in Hauser et al., 2011). ABA regulation may also happen at the level of RNA metabolism since a few components of the network, such as ABA HYPERSENSITIVE1 and CAP BINDING PROTEIN20, are known RNA binding proteins (Kuhn et al., 2008). Our work suggests that not only are a few components of the network involved in RNA metabolism, but the signaling components themselves are also targeted by SR45 for postsplicing regulation, since the transcripts of ~30% (43 out of the 147) of the ABA signaling genes are associated with SR45 (Supplemental Data Set 3). The SARs involved in the ABA response pathway are particularly enriched in the phosphatase and kinase and transcription factors categories, indicating that SR45 regulation occurs at major hubs of the network (Figure 5A) (Hauser et al., 2011). The role of SR45 in regulating SARs in the "phosphatase and kinase" node may be analogous to the role of Drosophila RNPS1 in the MAPK kinase pathway, albeit in Drosophila, the AS of MAPK kinase genes is regulated (Ashton-Beaucage et al., 2010; Roignant and Treisman, 2010) while in Arabidopsis, the regulation occurs in postsplicing processes, possibly through NMD, mRNA stability, and/or 3′-end formation (Lykke-Andersen et al., 2001; Wiegand et al., 2003). The regulation through postsplicing processes is likely true for the majority of the intron-containing SAR transcripts given that most are spliced mRNAs.

Despite the fact that AS is highly prevalent in plants and that regulated splicing plays an important role in plant growth, development, and stress responses, little is known about AS regulation (Reddy et al., 2013; Staiger and Brown, 2013). Furthermore, there are a large number (over 300) of different RNA binding proteins (RBPs) in plants (Silverman et al., 2013), but the global targets of most of these RBPs are not known. Our genome-wide identification of SR45-associated RNAs lays the foundation for further analysis of plant RBPs involved in mRNA processing.

METHODS

Plant Materials and Growth Conditions

The following *Arabidopsis thaliana* genotypes were used in this study: the wild type (Col), the SR45 mutant (*sr45-1*), the complemented transgenic line containing *35S:SR45.1-GFP* in *sr45-1* (*SR45.1-GFP*), and the transgenic line containing 35S:GFP (GFP). All lines were in the Arabidopsis ecotype Col background. The SR45.1-GFP transgenic line was a kind gift from X. Zhang (Zhang and Mount, 2009). The GFP line was described previously (Ali et al., 2003). The seeds used in this study for all the genotypes were harvested at the same time from plants grown under the same standard conditions (23°C; 16-h/8-h light/dark photoperiod; 120 μmol/m^2/s white fluorescence light). For immunoblotting, immunoprecipitation (IP), nuclear RNA sequencing, and RIP, the seedlings were prepared as following: seeds (50 mg) were surface-sterilized with 50% bleach and placed into 100 mL of Murashige and Skoog (MS) medium (0.5× MS basal salt, 2.5 mM MES, and 2% sucrose, pH 5.7) in a 250-mL flask. The seeds were kept in the dark at 4°C for 3 d and then moved to a growth chamber. The chamber was set at 23°C with a 16-h/8-h light/dark photoperiod. The flasks were kept on a shaker at 150 rpm. Ten-day-old seedlings were collected 4 h after dawn. The seedlings were rinsed with Nanopure water five times and wrapped in a few layers of Kimwipes to remove water. The seedlings were weighed, immediately frozen in liquid N_2, and stored at −80°C. For the RIP assay, the water-rinsed seedlings were cross-linked before being frozen. The cross-linking was performed by immersing the seedlings in 0.5% formaldehyde and applying a vacuum four times (15 s/time). The seedlings were then kept at room temperature for 10 min, and glycine was added to a final concentration of 83 mM. Following this, the seedlings were again subjected to vacuum four times (15 s/time) and incubated for 5 min to quench the cross-linking. The tissue was then rinsed, weighed, and frozen as described above.

Nuclear Extract Preparation

For immunoblot and IP assays, the nuclear extracts were prepared as described (Lawrence et al., 2004; Gilbert and Svejstrup, 2006). Briefly, 3 g of frozen seedlings was ground into a fine powder in liquid nitrogen and suspended in 25 mL of Honda buffer (1.25% Ficoll 400, 2.5% Dextran T40, 0.44 M sucrose, 10 mM $MgCl_2$, 0.5% Triton X-100, 20 mM HEPES KOH, pH 7.4, 5 mM DTT, 1 mM PMSF, and 1% protease inhibitor cocktail [P9599; Sigma-Aldrich]). The suspension was filtered through two layers of Miracloth into a 30-mL Corex tube. The filtrate was centrifuged at 3000*g* for 8 min at 4°C. The pellet containing nuclei was resuspended in 1 mL Honda buffer and centrifuged at 2500*g* for 5 min at 4°C. This washing step was

repeated two more times. The pellet was then resuspended in 500 μL nuclei lysis buffer (50 mM Tris-HCl, pH8.0, 10 mM EDTA, 1% SDS, 1 mM PMSF, and 1% protease inhibitor cocktail) by pipetting up and down and sonicated using a Covaris M220 Focused-ultrasonicator for 1 min at 7°C (peak power, 75; duty factor, 20; cycles/burst, 300). The extract was then centrifuged for 10 min at 16,000*g* at 4°C, and the supernatant was transferred to a fresh tube. DNA, RNA, and protein concentrations were measured using a NanoDrop to ensure a similar concentration across all samples. Aliquots (100 μL) of the nuclear extract for each sample were prepared, frozen in liquid nitrogen, and stored at −80°C.

For RIP assays, the nuclear extract was prepared as described above with RnaseOUT (Invitrogen) added to the Honda buffer (8 units/mL) and nuclei lysis buffer (160 units/mL).

IP and Immunoblotting

For IP assays, 100 μL of NE was diluted with 900 μL of IP dilution buffer (100 mM Tris-HCl, pH 7.5, 75 mM NaCl, 1 mM EDTA, 0.1% Triton X-100, and 1% protease inhibitor cocktail [P9599; Sigma-Aldrich]) and aliquoted into two tubes (500 μL/tube). One microgram of anti-GFP (1:500 dilution; JL-8; Clontech) or 1 μg anti-KCBP antibody (used as mock IP; 1:500 dilution) (Vos et al., 2000) was added to each tube and incubated at 4°C on a rotating wheel overnight. Ten microliters of protein A-conjugated Dynabeads (Life Technologies) was washed three times with 1 mL of IP dilution buffer and added to each sample. The samples were further incubated at 4°C for four more hours with rotation. The beads were washed three times with IP wash buffer (50 mM HEPES-KOH, pH 7.5, 300 mM KCl, 0.05% Nonidet P-40, 0.5 mM DTT, and 1% protease inhibitor cocktail) and three times with high-salt wash buffer (50 mM HEPES-KOH, pH 7.5, 500 mM KCl, 0.05% Nonidet P-40, 0.5 mM DTT, and 1% protease inhibitor cocktail). For each wash, 1 mL of wash buffer was added and the sample was rotated at 4°C for 5 min. The antibody-antigen complex was eluted with 30 μL of 1× SDS-PAGE loading buffer (10% [v/v] glycerol, 50 mM Tris-HCl, pH 6.8, 2 mM EDTA, 2% [w/v] SDS, 100 mM DTT, and 0.1% bromophenol blue) by heating at 70°C for 10 min. The eluate was resolved on a 12% SDS-PAGE gel, blotted, and probed with anti-GFP antibody (sc-8332; Santa Cruz Biotechnology) and detected with an enhanced chemiluminescence detection system.

RIP Assay

The RIP assay was performed as described (Lawrence et al., 2004; Gilbert and Svejstrup, 2006) with the anti-GFP antibody (JL-8; Clontech). Briefly, 100 μL of NE prepared from formaldehyde cross-linked seedlings was diluted with 900 μL of ChIP dilution buffer (1.1% Triton X-100, 1.2 mM EDTA, 16.7 mM Tris-HCl, pH 8, 167 mM NaCl, and 160 units/mL RnaseOUT) and centrifuged at 16,000*g* for 10 min at 4°C. The supernatant was transferred to a fresh Eppendorf tube, and 10 μL of the supernatant was taken out and kept on ice as RNA inputs. Thirty microliters of Protein A agarose/Salmon Sperm DNA (16-157; Upstate) beads for each RIP sample was prepared by washing the beads five times with 1 mL of binding/washing buffer (150 mM NaCl, 20 mM Tris HCl, pH 8.0, 2 mM EDTA, 1% Triton X-100, and 0.1% SDS). The beads were resuspended in 50 μL of binding/washing buffer. The beads and 1 μg of anti-GFP antibody (JL-8) were added to the diluted NE, and the samples were incubated on a rotator for 3 h at 4°C. The beads were then washed with 1 mL binding/washing buffer containing 40 units/ml RnaseOUT six times. For each wash, the beads were kept on a rotator at 4°C for 5 min and centrifuged at 2000 rpm for 2 min, and the supernatant was then removed. To elute the protein-RNA complexes, 60 μL of RIP elution buffer (100 mM Tris HCl, pH 8.0, 10 mM EDTA, 1% SDS, and 800 units/mL RnaseOUT) was added to the beads, and the tubes were incubated on a rotator at room temperature for 10 min. The beads were centrifuged at 4000 rpm for 1 min, and the supernatant was saved. The elution was repeated with an additional 60 μL of RIP elution buffer at 65°C with mixing (800 rpm) for 10 min. The samples were centrifuged and the supernatants from two elutions were combined. At the same time, 110 μL of RIP elution buffer was added to the 10 μL of RNA input sample. Then, 1.2 μL of 20 mg/mL Proteinase K was added to each IP or input sample. The tubes were incubated at 65°C for 1 h. The RNA was isolated using Trizol reagent (Life Technologies) following the manufacturer's instructions. To facilitate RNA precipitation, 20 μg of glycogen was added to the aqueous phase before the isopropanol precipitation. The RNA samples were further treated using a Turbo DNA-free kit (AM1907; Ambion) to remove DNA contamination and cleaned with an RNeasy MiniElute Kit (Qiagen) following the manufacturer's instructions. The RNA was eluted into 15 μL of RNase-free water.

RIP-Seq

RNA from RIP with SR45.1-GFP and Col nuclear extract was sequenced at Global Biologics. Briefly, the sequencing libraries were constructed using the NEBNext Ultra Directional RNA Library Prep Kit for Illumina. The libraries were bar-coded, pooled, and further sequenced using the Illumina sequencing platform NextSeq500 for Single Read 75-bp sequencing.

Nuclear RNA-Seq

Nuclear RNA was isolated from the NE of SR45.1-GFP and *sr45-1* using Trizol reagent, treated with TURBO DNA-free kit, and cleaned with an RNeasy MiniElute kit. The sequencing was performed at the Genome Sequencing and Analysis Core Resource, Duke University. Briefly, the RNA samples were processed with a Ribo-Zero rRNA removal kit (MRZPL116; Epicentre). The sequencing libraries were constructed from rRNA-depleted samples using a TruSeq RNA Library Prep Kit, bar-coded, pooled, and sequenced using the Illumina HiSeq platform for single end 50-bp sequencing.

RT-qPCR

DNase-treated RIP, nuclear RNA, or cytosolic RNA was reverse-transcribed using the SuperScript III first-strand synthesis system (18080-051; Life Technologies) using random hexamers and further quantified with qPCR using SYBR green master I (Roche) and gene-specific primers (Supplemental Data Set 8). For each RT-qPCR, at least three biological replicates were performed. A control reaction without adding reverse transcriptase was always performed for each RT and followed by qPCR to ensure that there was no genomic DNA contamination.

Analysis of Illumina Sequencing Data

The quality evaluation of the data, the data mapping to Arabidopsis genome and RPKM calculation for each transcript were performed using tools in iPlant (http://www.iplantcollaborative.org/ci/discovery-environment). Briefly, the fastq data were first evaluated for their quality using FastQC_0.10.1(multi-file). The high quality fastq data were then mapped to the TAIR10 genome using TopHat2-SE and the following parameter settings: reference genome, *Arabidopsis thaliana* [*Mouse-ear cress*] (*Ensembl 14*); reference annotations, *Arabidopsis thaliana* (*Mouse-ear cress*) (Ensembl 14); minimum length of read segments, 20; minimum isoform fraction, 0.15; Bowtie 2 speed and sensitivity, sensitive; maximum intron length that may be found during split-segment search, 10,000; minimum intron length, 50; Bowtie version, 2.1.0; anchor length, 8; number of mismatches allowed in each segment alignment for reads mapped independently, 2; maximum intron length, 5000; maximum number of mismatches that can appear in the anchor region of spliced alignment, 0;

maximum number of alignments to be allowed, 20; minimum intron length that may be found during split-segment search, 50; TopHat version, 2.0.9 (Kim et al., 2013). The bam files generated from TopHat analysis were further processed to remove the duplicate reads and reads aligned to multiple genomic positions using R scripts with Bioconductor packages as follows: the R code: *> library(GenomicAlignments); > library(GenomicRanges); > library(Rsamtools); > library(rtracklayer); > flag0 <- scanBamFlag(isDuplicate=FALSE, isNotPassingQualityControls=FALSE); > param0 <- ScanBamParam(flag=flag0, what="seq"); > ; > x <- readGAlignments("input.bam", use.names=TRUE, param=param0); > dup <- duplicated(mcols(x)$seq); > table(dup); > y <- x[!dup]; > export(y, BamFile("output.bam"))*. The mapped, unique, and nonredundant sequence reads (the processed bam files) were linked to and the RPKM was calculated for each TAIR10 gene and transcript using Cufflinks2 as follows: parameter setting: pre-mRNA fraction, 0.15; alpha value for the binomial test used during false positive spliced alignment filtration, 0.001; small anchor fraction, 0.09; minimum isoform fraction, 0.1; number of base pairs allowed to enter the intron of a transcript when determining if a read or another transcript is mappable with it, 8; normalized by the upper quartile of the number of fragments mapping to individual loci, TRUE; fraction of average coverage below which to trim the 3′ end of an assembled transcript, 0.1; minimum intron length, 50; number of importance samples generated for each locus during abundance estimation, 1000; minimum average coverage required to attempt 3′ trimming, 10; maximum genomic length allowed for a given bundle, 3,500,000; number of iterations allowed during MLE of abundances, 5000; minimum fragments per transfrag, 10; maximum intron length, 5000; Cufflinks version, 2.1.1 (Trapnell et al., 2012). The multiple GTF files generated from Cufflinks2 were further merged together using Cuffmerge2 with the following parameter settings: select reference genome annotation, *Arabidopsis thaliana* (*Mouse-ear cress*) (Ensembl 14); select reference genome sequence, *Arabidopsis thaliana* (*Mouse-ear cress*) (Ensembl 14); discard isoforms with abundance below this, 0.1; Cuffmerge version, 2.1.1. With the merged GTF as the annotation file, the processed bam files were reanalyzed using Cufflinks2 using the same parameters as above. The RPKM data of all transcripts were extracted from the output files "isoforms.fpkm_tracking" of the second round Cufflinks2 analysis. The genome-wide variation evaluation between and within treatments (RIP versus mock) was performed with the RPKM data of all the transcripts using R functions (plot(x, y) and lm(y~x)). To identify the enriched transcripts in the RIP-seq, the RPKM of each transcript was compared between RIP (SR45.1-GFP) and mock (Col) using Student's *t* test in Excel. The transcripts showing significant difference were further filtered based on the ratio of RIP to mock and the average abundance level of RIP replicates.

For the nuclear RNA-seq, the analysis was done essentially as above with the nuclear sequence data of SR45.1-GFP and *sr45-1* to identify the DE genes. For the identification of DP genes between SR45.1-GFP and *sr45-1*, the mapped nuclear RNA sequence data were processed with iDiffIR (http://combi.cs.colostate.edu/idiffir/).

GO and *cis*-Element Analysis

For GO enrichment analysis, the SAR genes were analyzed using GeneCoDis, AgriGO, and DAVID with the following parameter settings: reference list, all annotated genes in the *Arabidopsis* genome; statistical method, hypergeometric; method to correct P values for multiple hypothesis testing, false discovery rate (Carmona-Saez et al., 2007; Huang et al., 2009; Du et al., 2010).

For the de novo *cis*-element identification, MEME (Bailey et al., 2009) was used with the SAR gene sequences as input and non-SAR gene sequences as the background. The non-SAR genes were defined as those genes that were highly expressed in the nuclear seq data (FPKM > 20) and not enriched in the RIP assay. The gene sequences (fasta format) were extracted from the TAIR10 database (https://www.arabidopsis.org). Prior to MEME analysis, a position-specific priors (PSP) file was generated with the SAR and background gene sequences as inputs using the "psp-gen" program within the MEME-SUITE package (http://alternate.meme-suite.org) with default parameters. MEME was run on a cluster of Linux workstations with the following options: "-dna -mod zoops -minw 5 -maxw 10 -nmotifs 30 -psp v2.psp -evt 0.001 -maxsize 50000000" (v2.psp, the PSP file).

To identify the potential RNA motifs showing similarity to the *cis*-elements enriched in SAR genes, we searched the database "RNA binding motifs" (Laiho et al., 2013) using the TOMTOM tool of the MEME suite with the following command line: "tomtom -no-ssc -oc . -verbosity 1 -min-overlap 5 -dist pearson -evalue -thresh 0.05 meme.txt db/RNA/Ray2013_rbp_All_Species.meme" (meme.txt, the cis-elements enriched in SAR genes; db/RNA/Ray2013_rbp_All_Species.meme, RNA binding motif database).

To determine the position distribution of the RNA motifs relative to the basic structural features of SAR genes, we used an in-house R program (available upon request).

ABA Response of SR45 Mutant *sr45-1*

The seed germination and cotyledon greening tests were conducted using the methods described earlier (Robert et al., 2006). Briefly, surface-sterilized seeds were plated on solid MS medium (MS salt, 2.5 mM MES, 1% sucrose, pH 5.7, and 0.9% Phytagar) containing various concentrations of ABA (0, 1, 10, and 100 μM) in 15 × 100-mm Petri dishes. The dishes were incubated 3 d at 4°C and then transferred to a growth chamber set at 22°C in a 16/8-h light/dark photoperiod. The germination and cotyledon greening were scored 4 h after dawn daily. For the water loss test, the procedure described previously was followed (Verslues et al., 2006; Hua et al., 2012).

Accession Numbers

Sequence data from this article can be found in the SRA database of GenBank under accession number SRP041864 and in the TAIR database under the following accession numbers: AT1G15010, ERF012 (AT1G21910), AT1G22470, EXL1 (AT1G35140), HAB1 (AT1G72770), ERF013 (AT1G77640), AT2G01300, CMTA6 (AT3G16940), MYB77 (AT3G50060), SRK2D (AT3G50500), CML9 (AT3G51920), SR45 (AT1G16610), PYR1 (AT4G17870), (AT4G29780), SRK2E (AT4G33950), CMTA1 (AT5G09410), SAUR20 (AT5G18020), SAUR21 (AT5G18030), and SRK2I (AT5G66880).

Supplemental Data

Supplemental Figure 1. Flowchart of sequencing data analyses.

Supplemental Figure 2. Pairwise dot plots of RIP replicates between and within treatments.

Supplemental Figure 3. The effect of *SR45* mutation on cotyledon greening and seed germination.

Supplemental Figure 4. Primer design and IGB view of nuclear-seq and RIP-seq profile for SAR genes in the ABA signaling pathway.

Supplemental Figure 5. RT-qPCR quantification of the total and AS transcript levels of expanded SARs, as described for *HAB1* in Figure 4C.

Supplemental Figure 6. The purity of nuclear and cytosol fractions.

Supplemental Figure 7. RT-qPCR quantification of the total and AS transcript levels of expanded SARs in the nuclear RNA fraction, as described for the total cellular RNA fraction in Supplemental Figure 5.

Supplemental Figure 8. RT-qPCR quantification of the total and AS transcript levels of expanded SARs in the cytosolic RNA fraction, as described for the total cellular RNA fraction in Supplemental Figure 5.

Supplemental Figure 9. Distribution of enriched motifs within SAR gene features.

Supplemental Table 1. Mapping statistics of nuclear RNA-seq and RIP-seq data.

Supplemental Table 2. Chi-square test of SAR gene enrichment in each node of the ABA signaling pathway.

Supplemental Table 3. Evidence for alternative processing of SAR genes involved in the ABA signaling network.

Supplemental Table 4. Enriched *cis*-elements in SAR gene sequences.

Supplemental Data Set 1. SR45-associated RNAs.

Supplemental Data Set 2. Enriched GO terms in SAR genes based on the GeneCoDis assay.

Supplemental Data Set 3. SAR genes in each particular class of ABA signaling components.

Supplemental Data Set 4. Differentially expressed genes between SR45.1-GFP and the SR45 mutant, *sr45-1*.

Supplemental Data Set 5. SAR transcripts from intronless genes.

Supplemental Data Set 6. List of genes that were differentially processed between SR45.1-GFP and the SR45 mutant, *sr45-1*.

Supplemental Data Set 7. List of intronless SAR genes whose expression was altered in the nuclear seq data between SR45.1-GFP and the SR45 mutant, *sr45-1*.

Supplemental Data Set 8. PCR primers used in this study.

ACKNOWLEDGMENTS

This research was supported by grants from the National Science Foundation (ABI 0743097) and the Department of Energy (DE-SC0010733). We thank I. Day, F. Martin, and S. Palusa for their comments on the manuscript.

AUTHOR CONTRIBUTIONS

D.X. and A.S.N.R. designed the experiments and prepared the manuscript. D.X. preformed the experiments. D.X., Y.W., M.H., A.S.N.R., and A.B. performed the data analyses.

Received July 17, 2015; revised October 19, 2015; accepted November 3, 2015; published November 24, 2015.

REFERENCES

Abdel-Ghany, S.E., Müller-Moulé, P., Niyogi, K.K., Pilon, M., and Shikanai, T. (2005). Two P-type ATPases are required for copper delivery in *Arabidopsis thaliana* chloroplasts. Plant Cell **17:** 1233–1251.

Ali, G.S., Golovkin, M., and Reddy, A.S. (2003). Nuclear localization and in vivo dynamics of a plant-specific serine/arginine-rich protein. Plant J. **36:** 883–893.

Ali, G.S., Palusa, S.G., Golovkin, M., Prasad, J., Manley, J.L., and Reddy, A.S. (2007). Regulation of plant developmental processes by a novel splicing factor. PLoS One **2:** e471.

Ali, G.S., Prasad, K.V., Hanumappa, M., and Reddy, A.S. (2008). Analyses of in vivo interaction and mobility of two spliceosomal proteins using FRAP and BiFC. PLoS One **3:** e1953.

Ashton-Beaucage, D., Udell, C.M., Lavoie, H., Baril, C., Lefrançois, M., Chagnon, P., Gendron, P., Caron-Lizotte, O., Bonneil, E., Thibault, P., and Therrien, M. (2010). The exon junction complex controls the splicing of MAPK and other long intron-containing transcripts in Drosophila. Cell **143:** 251–262.

Ausin, I., Greenberg, M.V., Li, C.F., and Jacobsen, S.E. (2012). The splicing factor SR45 affects the RNA-directed DNA methylation pathway in Arabidopsis. Epigenetics **7:** 29–33.

Badolato, J., Gardiner, E., Morrison, N., and Eisman, J. (1995). Identification and characterisation of a novel human RNA-binding protein. Gene **166:** 323–327.

Bailey, T.L., Boden, M., Buske, F.A., Frith, M., Grant, C.E., Clementi, L., Ren, J., Li, W.W., and Noble, W.S. (2009). MEME SUITE: tools for motif discovery and searching. Nucleic Acids Res. **37:** W202–W208.

Brogna, S., and Wen, J. (2009). Nonsense-mediated mRNA decay (NMD) mechanisms. Nat. Struct. Mol. Biol. **16:** 107–113.

Calificе, S., Baurain, D., Hanikenne, M., and Motte, P. (2012). A single ancient origin for prototypical serine/arginine-rich splicing factors. Plant Physiol. **158:** 546–560.

Carmona-Saez, P., Chagoyen, M., Tirado, F., Carazo, J.M., and Pascual-Montano, A. (2007). GENECODIS: a web-based tool for finding significant concurrent annotations in gene lists. Genome Biol. **8:** R3.

Carvalho, R.F., Carvalho, S.D., and Duque, P. (2010). The plant-specific SR45 protein negatively regulates glucose and ABA signaling during early seedling development in Arabidopsis. Plant Physiol. **154:** 772–783.

Cléry, A., Jayne, S., Benderska, N., Dominguez, C., Stamm, S., and Allain, F.H. (2011). Molecular basis of purine-rich RNA recognition by the human SR-like protein Tra2-β1. Nat. Struct. Mol. Biol. **18:** 443–450.

Day, I.S., Golovkin, M., Palusa, S.G., Link, A., Ali, G.S., Thomas, J., Richardson, D.N., and Reddy, A.S. (2012). Interactions of SR45, an SR-like protein, with spliceosomal proteins and an intronic sequence: insights into regulated splicing. Plant J. **71:** 936–947.

Du, Z., Zhou, X., Ling, Y., Zhang, Z., and Su, Z. (2010). agriGO: a GO analysis toolkit for the agricultural community. Nucleic Acids Res. **38:** W64–W70.

Fairbrother, W.G., Yeh, R.F., Sharp, P.A., and Burge, C.B. (2002). Predictive identification of exonic splicing enhancers in human genes. Science **297:** 1007–1013.

Feng, Y., Valley, M.T., Lazar, J., Yang, A.L., Bronson, R.T., Firestein, S., Coetzee, W.A., and Manley, J.L. (2009). SRp38 regulates alternative splicing and is required for Ca(2+) handling in the embryonic heart. Dev. Cell **16:** 528–538.

Filichkin, S.A., Cumbie, J.S., Dharmawardhana, P., Jaiswal, P., Chang, J.H., Palusa, S.G., Reddy, A.S., Megraw, M., and Mockler, T.C. (2015). Environmental stresses modulate abundance and timing of alternatively spliced circadian transcripts in Arabidopsis. Mol. Plant **8:** 207–227.

Gatfield, D., and Izaurralde, E. (2002). REF1/Aly and the additional exon junction complex proteins are dispensable for nuclear mRNA export. J. Cell Biol. **159:** 579–588.

Gatfield, D., Unterholzner, L., Ciccarelli, F.D., Bork, P., and Izaurralde, E. (2003). Nonsense-mediated mRNA decay in Drosophila: at the intersection of the yeast and mammalian pathways. EMBO J. **22:** 3960–3970.

Gilbert, C., and Svejstrup, J.Q. (2006). RNA immunoprecipitation for determining RNA-protein associations in vivo. In Current Protocols in Molecular Biology, F.M. Ausubel, R. Brent, R.E. Kingston, D.D. Moore, J.G. Seidman, J.A. Smith, and K. Struhl, eds (New York: Wiley), pp. 27.4.1–27.4.11.

Golovkin, M., and Reddy, A.S. (1999). An SC35-like protein and a novel serine/arginine-rich protein interact with Arabidopsis U1-70K protein. J. Biol. Chem. **274:** 36428–36438.

Harada, K., Yamada, A., Yang, D., Itoh, K., and Shichijo, S. (2001). Binding of a SART3 tumor-rejection antigen to a pre-mRNA splicing

factor RNPS1: a possible regulation of splicing by a complex formation. Int. J. Cancer **93:** 623–628.

Hauser, F., Waadt, R., and Schroeder, J.I. (2011). Evolution of abscisic acid synthesis and signaling mechanisms. Curr. Biol. **21:** R346–R355.

Hoskins, A.A., and Moore, M.J. (2012). The spliceosome: a flexible, reversible macromolecular machine. Trends Biochem. Sci. **37:** 179–188.

Hua, D., Wang, C., He, J., Liao, H., Duan, Y., Zhu, Z., Guo, Y., Chen, Z., and Gong, Z. (2012). A plasma membrane receptor kinase, GHR1, mediates abscisic acid- and hydrogen peroxide-regulated stomatal movement in Arabidopsis. Plant Cell **24:** 2546–2561.

Huang, W., Sherman, B.T., and Lempicki, R.A. (2009). Systematic and integrative analysis of large gene lists using DAVID bioinformatics resources. Nat. Protoc. **4:** 44–57.

Jurica, M.S., and Moore, M.J. (2003). Pre-mRNA splicing: awash in a sea of proteins. Mol. Cell **12:** 5–14.

Kalsotra, A., and Cooper, T.A. (2011). Functional consequences of developmentally regulated alternative splicing. Nat. Rev. Genet. **12:** 715–729.

Kaneko, S., and Manley, J.L. (2005). The mammalian RNA polymerase II C-terminal domain interacts with RNA to suppress transcription-coupled 3′ end formation. Mol. Cell **20:** 91–103.

Kataoka, N., and Dreyfuss, G. (2004). A simple whole cell lysate system for in vitro splicing reveals a stepwise assembly of the exon-exon junction complex. J. Biol. Chem. **279:** 7009–7013.

Kim, B., Kang, S., and Kim, S.J. (2013). Genome-wide pathway analysis reveals different signaling pathways between secreted lactoferrin and intracellular delta-lactoferrin. PLoS One **8:** e55338.

Kim, S.H., Koroleva, O.A., Lewandowska, D., Pendle, A.F., Clark, G.P., Simpson, C.G., Shaw, P.J., and Brown, J.W. (2009). Aberrant mRNA transcripts and the nonsense-mediated decay proteins UPF2 and UPF3 are enriched in the Arabidopsis nucleolus. Plant Cell **21:** 2045–2057.

Kimura, T., Hashimoto, I., Nishizawa, M., Ito, S., and Yamada, H. (2010). Novel cis-active structures in the coding region mediate CRM1-dependent nuclear export of IFN-α 1 mRNA. Med. Mol. Morphol. **43:** 145–157.

Koroleva, O.A., Calder, G., Pendle, A.F., Kim, S.H., Lewandowska, D., Simpson, C.G., Jones, I.M., Brown, J.W., and Shaw, P.J. (2009). Dynamic behavior of Arabidopsis eIF4A-III, putative core protein of exon junction complex: fast relocation to nucleolus and splicing speckles under hypoxia. Plant Cell **21:** 1592–1606.

Kuhn, J.M., Hugouvieux, V., and Schroeder, J.I. (2008). mRNA cap binding proteins: effects on abscisic acid signal transduction, mRNA processing, and microarray analyses. Curr. Top. Microbiol. Immunol. **326:** 139–150.

Laiho, A., Kotaja, N., Gyenesei, A., and Sironen, A. (2013). Transcriptome profiling of the murine testis during the first wave of spermatogenesis. PLoS One **8:** e61558.

Lawrence, R.J., Earley, K., Pontes, O., Silva, M., Chen, Z.J., Neves, N., Viegas, W., and Pikaard, C.S. (2004). A concerted DNA methylation/histone methylation switch regulates rRNA gene dosage control and nucleolar dominance. Mol. Cell **13:** 599–609.

Le Hir, H., Gatfield, D., Izaurralde, E., and Moore, M.J. (2001). The exon-exon junction complex provides a binding platform for factors involved in mRNA export and nonsense-mediated mRNA decay. EMBO J. **20:** 4987–4997.

Le Hir, H., Izaurralde, E., Maquat, L.E., and Moore, M.J. (2000). The spliceosome deposits multiple proteins 20-24 nucleotides upstream of mRNA exon-exon junctions. EMBO J. **19:** 6860–6869.

Lee, S.C., and Luan, S. (2012). ABA signal transduction at the crossroad of biotic and abiotic stress responses. Plant Cell Environ. **35:** 53–60.

Li, C., Lin, R.I., Lai, M.C., Ouyang, P., and Tarn, W.Y. (2003). Nuclear Pnn/DRS protein binds to spliced mRNPs and participates in mRNA processing and export via interaction with RNPS1. Mol. Cell. Biol. **23:** 7363–7376.

Li, X., Niu, T., and Manley, J.L. (2007). The RNA binding protein RNPS1 alleviates ASF/SF2 depletion-induced genomic instability. RNA **13:** 2108–2115.

Long, J.C., and Caceres, J.F. (2009). The SR protein family of splicing factors: master regulators of gene expression. Biochem. J. **417:** 15–27.

Lykke-Andersen, J., Shu, M.D., and Steitz, J.A. (2001). Communication of the position of exon-exon junctions to the mRNA surveillance machinery by the protein RNPS1. Science **293:** 1836–1839.

Mayeda, A., Badolato, J., Kobayashi, R., Zhang, M.Q., Gardiner, E.M., and Krainer, A.R. (1999). Purification and characterization of human RNPS1: a general activator of pre-mRNA splicing. EMBO J. **18:** 4560–4570.

McCracken, S., Longman, D., Johnstone, I.L., Cáceres, J.F., and Blencowe, B.J. (2003). An evolutionarily conserved role for SRm160 in 3′-end processing that functions independently of exon junction complex formation. J. Biol. Chem. **278:** 44153–44160.

Michelle, L., et al. (2012). Proteins associated with the exon junction complex also control the alternative splicing of apoptotic regulators. Mol. Cell. Biol. **32:** 954–967.

Mili, S., and Steitz, J.A. (2004). Evidence for reassociation of RNA-binding proteins after cell lysis: implications for the interpretation of immunoprecipitation analyses. RNA **10:** 1692–1694.

Miyagawa, R., Tano, K., Mizuno, R., Nakamura, Y., Ijiri, K., Rakwal, R., Shibato, J., Masuo, Y., Mayeda, A., Hirose, T., and Akimitsu, N. (2012). Identification of cis- and trans-acting factors involved in the localization of MALAT-1 noncoding RNA to nuclear speckles. RNA **18:** 738–751.

Nagel, R.J., Lancaster, A.M., and Zahler, A.M. (1998). Specific binding of an exonic splicing enhancer by the pre-mRNA splicing factor SRp55. RNA **4:** 11–23.

Nemhauser, J.L., Hong, F., and Chory, J. (2006). Different plant hormones regulate similar processes through largely nonoverlapping transcriptional responses. Cell **126:** 467–475.

Nogués, G., Muñoz, M.J., and Kornblihtt, A.R. (2003). Influence of polymerase II processivity on alternative splicing depends on splice site strength. J. Biol. Chem. **278:** 52166–52171.

Nott, A., Le Hir, H., and Moore, M.J. (2004). Splicing enhances translation in mammalian cells: an additional function of the exon junction complex. Genes Dev. **18:** 210–222.

Palusa, S.G., Ali, G.S., and Reddy, A.S. (2007). Alternative splicing of pre-mRNAs of Arabidopsis serine/arginine-rich proteins: regulation by hormones and stresses. Plant J. **49:** 1091–1107.

Pertea, M., Mount, S.M., and Salzberg, S.L. (2007). A computational survey of candidate exonic splicing enhancer motifs in the model plant *Arabidopsis thaliana*. BMC Bioinformatics **8:** 159.

Popp, M.W., and Maquat, L.E. (2013). Organizing principles of mammalian nonsense-mediated mRNA decay. Annu. Rev. Genet. **47:** 139–165.

Reddy, A.S., and Shad Ali, G. (2011). Plant serine/arginine-rich proteins: roles in precursor messenger RNA splicing, plant development, and stress responses. Wiley Interdiscip. Rev. RNA **2:** 875–889.

Reddy, A.S.N., Marquez, Y., Kalyna, M., and Barta, A. (2013). Complexity of the alternative splicing landscape in plants. Plant Cell **25:** 3657–3683.

Reichert, V.L., Le Hir, H., Jurica, M.S., and Moore, M.J. (2002). 5′ Exon interactions within the human spliceosome establish a framework for exon junction complex structure and assembly. Genes Dev. **16:** 2778–2791.

Robert, N., Merlot, S., N'guyen, V., Boisson-Dernier, A., and Schroeder, J.I. (2006). A hypermorphic mutation in the protein phosphatase 2C HAB1 strongly affects ABA signaling in Arabidopsis. FEBS Lett. **580:** 4691–4696.

Roignant, J.Y., and Treisman, J.E. (2010). Exon junction complex subunits are required to splice Drosophila MAP kinase, a large heterochromatic gene. Cell **143:** 238–250.

Sakashita, E., Tatsumi, S., Werner, D., Endo, H., and Mayeda, A. (2004). Human RNPS1 and its associated factors: a versatile alternative pre-mRNA splicing regulator in vivo. Mol. Cell. Biol. **24:** 1174–1187.

Silverman, I.M., Li, F., and Gregory, B.D. (2013). Genomic era analyses of RNA secondary structure and RNA-binding proteins reveal their significance to post-transcriptional regulation in plants. Plant Sci. **205-206:** 55–62.

Singh, G., Kucukural, A., Cenik, C., Leszyk, J.D., Shaffer, S.A., Weng, Z., and Moore, M.J. (2012). The cellular EJC interactome reveals higher-order mRNP structure and an EJC-SR protein nexus. Cell **151:** 750–764.

Staiger, D., and Brown, J.W. (2013). Alternative splicing at the intersection of biological timing, development, and stress responses. Plant Cell **25:** 3640–3656.

Tacke, R., Tohyama, M., Ogawa, S., and Manley, J.L. (1998). Human Tra2 proteins are sequence-specific activators of pre-mRNA splicing. Cell **93:** 139–148.

Tange, T.O., Nott, A., and Moore, M.J. (2004). The ever-increasing complexities of the exon junction complex. Curr. Opin. Cell Biol. **16:** 279–284.

Thomas, J., Palusa, S.G., Prasad, K.V., Ali, G.S., Surabhi, G.K., Ben-Hur, A., Abdel-Ghany, S.E., and Reddy, A.S. (2012). Identification of an intronic splicing regulatory element involved in auto-regulation of alternative splicing of SCL33 pre-mRNA. Plant J. **72:** 935–946.

Trapnell, C., Roberts, A., Goff, L., Pertea, G., Kim, D., Kelley, D.R., Pimentel, H., Salzberg, S.L., Rinn, J.L., and Pachter, L. (2012). Differential gene and transcript expression analysis of RNA-seq experiments with TopHat and Cufflinks. Nat. Protoc. **7:** 562–578.

Trembley, J.H., Tatsumi, S., Sakashita, E., Loyer, P., Slaughter, C.A., Suzuki, H., Endo, H., Kidd, V.J., and Mayeda, A. (2005). Activation of pre-mRNA splicing by human RNPS1 is regulated by CK2 phosphorylation. Mol. Cell. Biol. **25:** 1446–1457.

Verslues, P.E., Agarwal, M., Katiyar-Agarwal, S., Zhu, J., and Zhu, J.K. (2006). Methods and concepts in quantifying resistance to drought, salt and freezing, abiotic stresses that affect plant water status. Plant J. **45:** 523–539.

Vos, J.W., Safadi, F., Reddy, A.S., and Hepler, P.K. (2000). The kinesin-like calmodulin binding protein is differentially involved in cell division. Plant Cell **12:** 979–990.

Wang, X., et al. (2012). SKIP is a component of the spliceosome linking alternative splicing and the circadian clock in Arabidopsis. Plant Cell **24:** 3278–3295.

Wang, Y., Xiao, X., Zhang, J., Choudhury, R., Robertson, A., Li, K., Ma, M., Burge, C.B., and Wang, Z. (2013). A complex network of factors with overlapping affinities represses splicing through intronic elements. Nat. Struct. Mol. Biol. **20:** 36–45.

Wiegand, H.L., Lu, S., and Cullen, B.R. (2003). Exon junction complexes mediate the enhancing effect of splicing on mRNA expression. Proc. Natl. Acad. Sci. USA **100:** 11327–11332.

Wu, H.P., Su, Y.S., Chen, H.C., Chen, Y.R., Wu, C.C., Lin, W.D., and Tu, S.L. (2014). Genome-wide analysis of light-regulated alternative splicing mediated by photoreceptors in *Physcomitrella patens*. Genome Biol. **15:** R10.

Wu, S., Romfo, C.M., Nilsen, T.W., and Green, M.R. (1999). Functional recognition of the 3′ splice site AG by the splicing factor U2AF35. Nature **402:** 832–835.

Zhang, J., Sun, X., Qian, Y., and Maquat, L.E. (1998). Intron function in the nonsense-mediated decay of beta-globin mRNA: indications that pre-mRNA splicing in the nucleus can influence mRNA translation in the cytoplasm. RNA **4:** 801–815.

Zhang, X.N., Mo, C., Garrett, W.M., and Cooper, B. (2014). Phosphothreonine 218 is required for the function of SR45.1 in regulating flower petal development in Arabidopsis. Plant Signal. Behav. **9:** e29134.

Zhang, X.N., and Mount, S.M. (2009). Two alternatively spliced isoforms of the Arabidopsis SR45 protein have distinct roles during normal plant development. Plant Physiol. **150:** 1450–1458.

Zorio, D.A., and Blumenthal, T. (1999). Both subunits of U2AF recognize the 3′ splice site in *Caenorhabditis elegans*. Nature **402:** 835–838.